J Mater Sci (2018) 53:215–229

Biomaterials

Self-antibacterial UV-curable waterborne polyurethane with pendant amine and modified by guanidinoacetic acid

Shuo Du[1], Yaya Wang[1], Caixia Zhang[1], Xiulin Deng[1], Xiaohu Luo[1], Yuxiang Fu[1], and Yali Liu[1,*]

[1] State Key Laboratory of Chemo/Biosensing and Chemometrics, College of Chemistry and Chemical Engineering, Hunan University, 2 Lushan South Road, Changsha 410082, People's Republic of China

Received: 17 May 2017
Accepted: 29 August 2017
Published online: 5 September 2017

© Springer Science+Business Media, LLC 2017

ABSTRACT

Enhancing the dispersion stability and self-antibacterial properties of cationic waterborne polyurethane materials is of vital importance to its various applications. In this work, a novel UV-curable waterborne polyurethane with pendant amine (PWPU) from 4-NCO prepolymer and modified by guanidinoacetic acid (GAA) was prepared by a simple method. The 4-NCO prepolymer is originated from the progressively grafting of tridentate polycaprolactone. The GAA, which is rarely used in coating industry, plays a positive reinforced role in our self-antibacterial coatings. Taking fully advantage of the merits of pendant amine and GAA, PWPU without bactericides possesses excellent properties in gram-negative (92.05%) and gram-positive (94.77%) antibacterial tests. Compared with the linear amine waterborne polyurethane (LWPU), PWPU has significant superiority in stability, and the increase in antibacterial efficiency is about 50%. Moreover, antibacterial efficiency still maintained 87.94% after 12 times washing. AFM results display that GAA and pendant amine increase the hydrophilic groups of coating surface, which improves the antibacterial performance. The experiments of thermal, mechanical performance and chemical resistance proof the reliability of the coatings. Therefore, this work has large potential in the applications of antibacterial materials.

Introduction

With the escalation of hygiene requirements, the antibacterial coatings have been extensively applied in medical equipment, oil storage, children's toys, furniture and other fields [1–5]. Most antibacterial coatings are functionalized by the addition of extra antibacterial agents such as triclosan, peroxides, silver ions, guanidine compounds and quaternary ammonium salts (QAS) [6–12]. However, those antibacterial coatings have been brought many

Address correspondence to E-mail: yaliliu@hnu.edu.cn

DOI 10.1007/s10853-017-1527-2

controversies, such as toxicity, pollution, high cost, drug resistance and unsustainable antibacterial activity, which restrict their service durability and scope of application [1, 3–6].

Nowadays, there have been attracted considerable attentions on self-antibacterial coatings due to their beneficial antibacterial property and durability. For instance, Garrison et al. [13] prepared cationic polyurethane and studied the effects of amine ratio on antibacterial properties. Ho et al. [14] developed an integrated self-antibacterial coating, in which the polyethylene glycol has anti-adhesion effect for bacteria. It has also been reported that the introduction of small molecular QAS into coating polymers by chemical grafting can bring about the dissolution of bacterial membranes [15, 16]. Furthermore, since the guanidine is prone to produce more formidable double hydrogen bonds with the bacteria membrane, several investigators employed guanidine polymers to construct the self-antibacterial coatings, and the effects of antibacterial groups' location were also investigated [17–20].

Among various strategies, cationic UV-curable waterborne polyurethane as a widely available material is a competitive solution due to the inherent QAS structure, favorable biocompatibility, environmental friendly, rapid cross-linking and outstanding performance [3, 21–23]. Currently, the polyurethane antibacterial coatings are typically prepared by a conventional method of incorporating amine groups into the polymer backbone. However, there exist three major drawbacks of current method: the limited antibacterial performances, complicated synthetic process and instability of dispersions [24]. Fortunately, attributed to the chemical features, polyurethane is suitable for the customization of molecule structure to acquire a stable dispersion and better antibacterial effect. Meanwhile, guanidinoacetic acid (GAA) is a derivative of glycine, which is innocuous, inexpensive and conveniently available, and is currently employed as feed additives in livestock cultivation [25]. However, so far a study of GAA in coating antibacterial performance has been rarely reported and such research is thus highly meaningful.

Herein, we present a novel self-antibacterial UV-curable PWPU and modified by GAA via a simple method to address the above challenges. The 4-NCO prepolymer was prepared at first step. Then, other materials with –OH were mixed to terminate in a single step. Neutralized PWPU was obtained after the addition of the acetic acid and GAA. This strategy is based on cationic polyurethane which links the GAA to the pendant position of whole chain to form macromolecular QAS, which containing guanidine and supplemented by polyethylene glycols. Those antibacterial parts work together to achieve reproducible and self-antibacterial effects. By the characterization, detection and comparison of PWPU and LWPU, PWPU has remarkable superiority on stability, and the increase in antibacterial efficiency is about 50%. As the method has advantages on simple, cheap and green, this work not only provides a new idea for preparing PWPU but also has large potential in the applications of antibacterial materials.

Experimental

Materials

Isophorone diisocyanate (IPDI, 222.3 g mol^{-1}, Industrial grade) was purchased from Covestro Greater Co., China (Shanghai, China). Polycaprolactone triol (PCL3050, 500 g mol^{-1}, Industrial grade) and polycaprolactone diol (PCL2054, 500 g mol^{-1}; PCL2000, 2000 g mol^{-1}, Industrial grade) were supplied by Pestorp Co., UK (Warrington, UK). Bicat8113 was provided by Shepherd China Rep., office (Shanghai, China). *N*,*N*-dimethyl ethanolamine (DMEA, 89.1 g mol^{-1}), *N*-methyldiethanolamine (MDEA, 119.1 g mol^{-1}), acetic acid (HAc, 60 g mol^{-1}), ethyl acetate (EA, 88.1 g mol^{-1}), methoxypolyethylene glycols (MPEG, 350 g mol^{-1}), β-hydroxyethyl methacrylate (HEMA, 130.1 g mol^{-1}), Darocur 1173 (photo-initiator, Industrial grade), guanidinoacetic acid (GAA, 117.1 g mol^{-1}) and other reagents were purchased from Sino pharm Chemical Reagent Co., China (Shanghai, China). *Escherichia coli* (*E. coli*) and *Bacillus subtilis* (*B. subtilis*) were purchased from HKM Co., Ltd (Guangdong, China). Deionized water was homemade. All drugs that are not specifically indicated are analytical grade, and reagents and containers involved in synthesis must be dried.

Synthesis of waterborne polyurethane resins

Preparation of PWPU

The synthesis process of PWPU and PUDs is shown in Fig. 1. A four-necked flask equipped with N_2

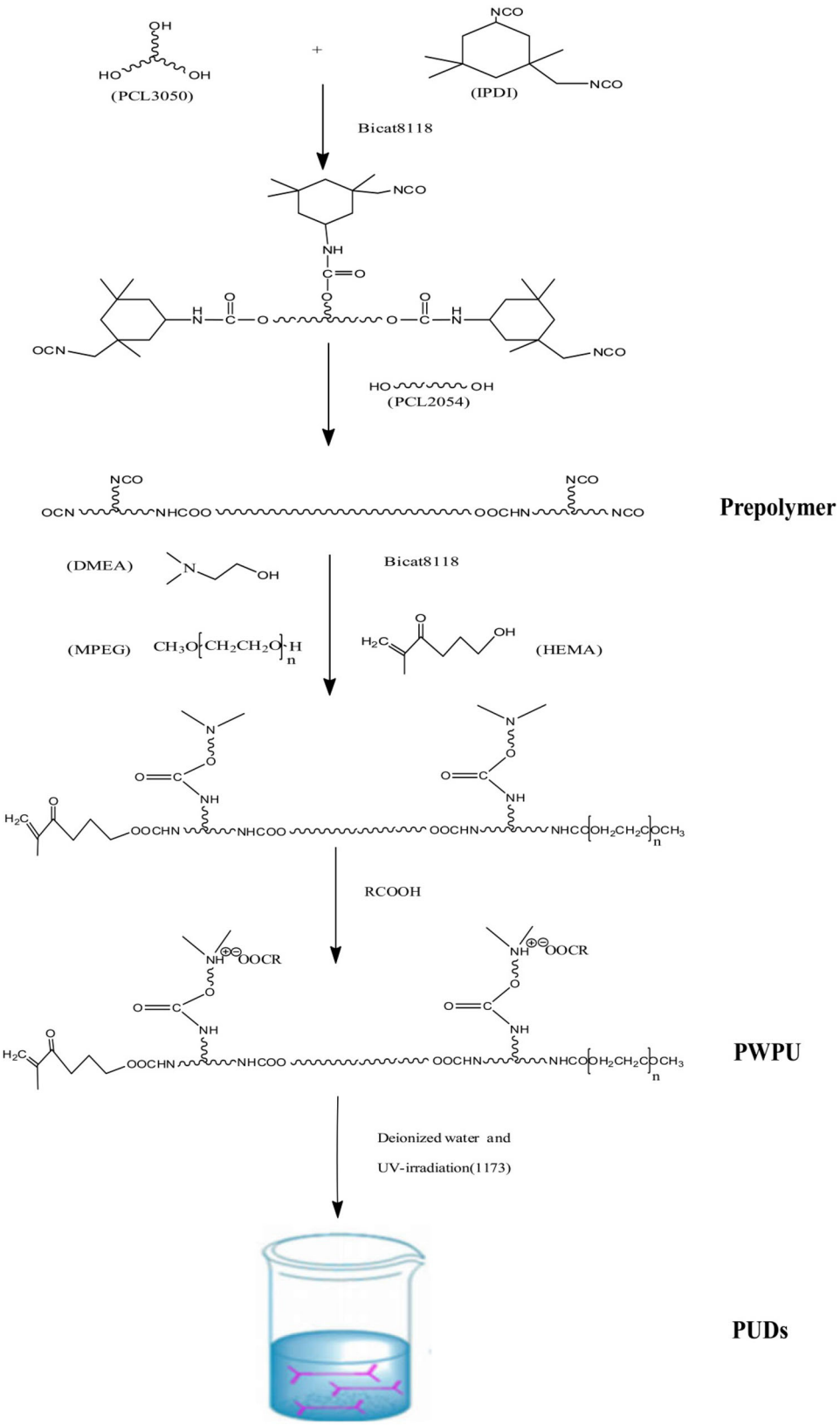

Figure 1 Synthesis process of the PWPU resin and PUDs.

Table 1 Basic information of waterborne polyurethane resins

Resins	PWPU-A	PWPU-B	PWPU-C	PWPU-D	LWPU-E
DMEA(MDEA):MPEG:HEMA (mol)	2:0:2	2:0.5:1.5	2:1:1	2:1.5:0.5	2:0:2
Functionality of double bonds	4	1.5	1	0.5	2
Functionality of –NCO	4	4	4	4	2
Functionality of –NR3	2	2	2	2	2
Theoretical Mn (g mol^{-1})	3272	3382	3492	3602	3388
Experimental Mn (g mol^{-1})	4009	3872	3734	3826	3865
Theoretical double bond contents (mol)	7.952%	5.770%	3.726%	1.806%	7.680%
Experimental double bond contents (mol)	7.577%	5.676%	3.645%	1.781%	7.393%
Theoretical Amine values (mgKOH g mol^{-1})	24.45	23.65	22.91	22.21	23.61
Experimental Amine values (mgKOH g mol^{-1})	19.21	18.98	18.53	18.46	21.33

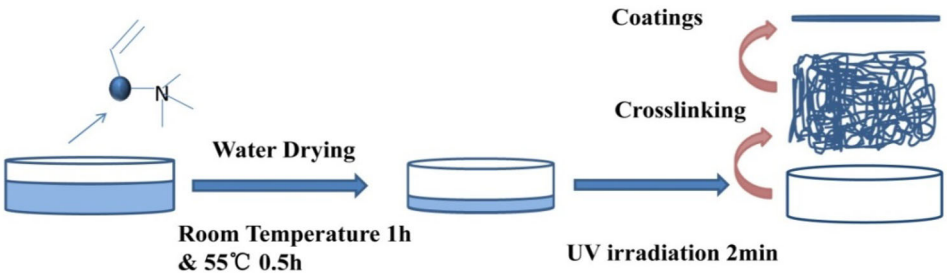

Figure 2 Preparation of coatings.

atmosphere, reflux condenser, mechanical stirrer and a thermometer was charged with IPDI and half of Bicat8118. The mixture was stirred and heated to 70 °C, and the initial –NCO value was measured. PCL3050 dissolved in EA was dropped into the solution within 2 h, and the –NCO value was continuously measured until it reached half of initial value. Then, PCL2050 was mixed in, and the reaction was carried out for further 2 h to produce the 4 –NCO prepolymer. After –NCO value reached the one-third of initial value, the temperature was cooled to 55 °C. The mixture of DMEA, MPEG, HEMA and other Bicat8118 was dropped for 5 h to ensure that the –NCO could not be detected. Finally, HAc (80% neutralization degree) was added into the container and stirred at 25 °C for 1 h. The colorless and transparent PWPU resin was obtained.

Preparation of the LWPU

The LWPU was synthesized by conventional methods while ensuring that the amine group was identical with PWPU. A same four-necked flask was charged with IPDI, PCL2000, Bicat8118 and EA under the N_2 atmosphere. The mixture was stirred and heated at 70 °C for 1 h for pre-polymerization. Then, MDEA was slowly dropped into the flask to extend the chain at 55 °C for 3 h. When –NCO value reached one-fourth of the initial value, HEMA was dropped into the flask to terminate for further 3 h. The –NCO value in synthesis, final amine value and double bond contents of resins were determined according to HG/T2409-92, ISO 25761-2014, GB/T 601-2002 and GB 1676-81, respectively. The Mn was measured by GPC (10-mg sample was dissolved in 1 ml of THF and measured at 40 °C). Afterward, the HAc (80% neutralization degree) was added and stirred at 25 °C for 1 h. The basic information of waterborne polyurethane resin is listed in Table 1.

Preparation of PUDs and coatings

The dispersions (30 wt%) were prepared by adding the resins, Darocur 1173 (4 wt% of monomer) and deionized water into a dispersion vessel with stirring for 1 h at room temperature. The solvent in the dispersion was distilled off by vacuum distillation. Then, the dispersions were prepared and named as PUD-A, PUD-B, PUD-C, PUD-D and PUD-E, respectively.

As shown in Fig. 2, 10 mL PUDs was poured in glass dishes (φ 90 mm), coated by the rod and dried at 25 °C for 1 h. Then, the coated dishes were transferred to oven, slowly heated and baked at 55 °C for

0.5 h. After evaporation of water, the dishes were moved to the UV curing machine for curing in 2 min. UV lamp has main wavelength of 365 nm, 1000 W power, UV energy 1000 J s^{-1}. The center of UV light from the film sample is 10 cm, and conveyor speed is 20 m min^{-1}. The coatings were named serially as F_A, F_B, F_C, F_D and F_E.

0, 0.25, 0.5, 0.75 and 1% GAA (wt. of the dispersion) were added to PUD-B, and those dispersions were called sequentially as PUD-B_1, PUD-B_2, PUD-B_3, PUD-B_4 and PUD-B_5 while coatings designated as B_1, B_2, B_3, B_4 and B_5.

Antibacterial experiments

Antibacterial experiments of PUDs

The *E. coli* (gram-negative) and *B. subtilis* (gram-positive) bacteria have a special ultraviolet absorption at 600 nm, which is used to evaluate the antibacterial properties of PUDs. The PUD-E and PUD-$B_{X\ (X:\ 1,\ 2,\ 3,\ 4\ and\ 5)}$ were selected to test. One milliliter of second-generation bacteria suspension with an OD_{600} values of 0.5–0.8 (contained nutrient solution) was aspirated into sterilized tube, and the original OD_{600} value was determined as blank control. Fifty microliters of PUD-B_X was added into the bacteria suspension and incubated at 4 °C for 2 h. The OD_{600} values were determined to compute the antibacterial efficiency of PUDs.

Antibacterial experiments of coatings

The $B_{X\ (X:\ 1,\ 2,\ 3,\ 4\ and\ 5)}$ and F_E coatings were detected for colony forming units on PTFE petri dish (ϕ 90 mm, 10 g of peptone, 10 g of NaCl, 5 g of yeast extract, 15 g of agar, pH 7.0). Three-milliliter bacterial suspension was injected into a sterile and uncoated PTFE petri dish and incubated at 37 °C for 4 h as blank control. Then, another 3 mL bacterial suspension was added to well-coated petri dishes of PWPU-B (B_X) and LWPU-E (F_E) coatings and incubated with cover at 37 °C for 4 h. After that, the bacterial suspension was diluted to a suitable concentration (1×10^6 cells mL^{-1}); 50 μL diluted suspension was coated on petri dishes which were numbered and cultured with cover in a shaker at 37 °C for 24 h. After incubation, the colony forming units (CFU) were calculated.

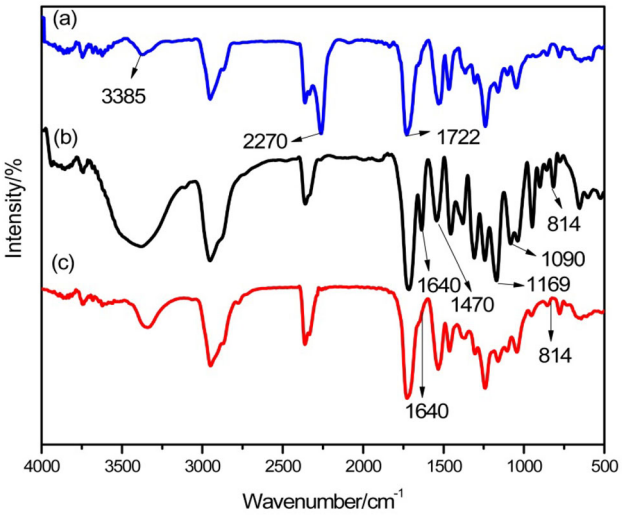

Figure 3 FTIR spectra of *a* 4-NCO prepolymer, *b* PWPU resin and *c* coatings.

Repeat antibacterial challenges

The repeat antibacterial challenges of coatings were carried out by washing with water [1, 8]. Firstly, the *B. subtilis* suspension was incubated with B_5 coating at 37 °C for 4 h and then washed the dishes by running water for next antibacterial test. The OD_{600} values of bacterial suspensions were determined before and after the incubation of each test.

Characterization methods

Characterization of the PUDs

The particle size and distribution were measured by laser diffraction particle size (Mastersizer-2000, Malvern, UK), with the range of 0.4–10000 nm.

The zeta potential of the PUDs was tested by laser zeta potentiometer (Mastersizer-2000, Malvern, UK).

The UV absorption spectra were determined by the UV–Vis (UV2450, Hitachi, Japan).

The filtered PUDs was added to a tube and centrifuged at 3000 r min^{-1} for 30 min in a high-speed centrifuge (TG16MW, Hexi, China). Then, it was allowed to stand for 24 h to observe whether the dispersion had been precipitated or delaminated.

According to GB/T6753.3-1986, the PUDs were placed in an oven at 50 ± 2 °C for 30 d to test the storage stability.

The OD_{600} values of PUDs and bacterial suspensions were determined by UV–Vis (UV2450, Hitachi,

Table 2 Basic properties and stability tests for PUDs

PUDs	PUD-A	PUD-B	PUD-C	PUD-D	PUD-E
DMEA(MDEA):MPEG:HEMA (mol)	2:0:2	2:0.5:1.5	2:1:1	2:1.5:0.5	2:0:2
Solids content (%)	32.04	31.56	31.49	31.93	31.40
Appearance					
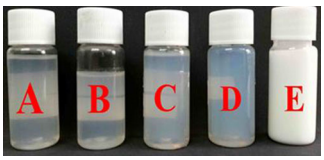	Transparent, slightly blue	Transparent, slightly blue	Transparent, slightly blue	Transparent, blue	Milky, white
Storage stability	Slightly layered	Stable	Stable	Stable	Layered
Centrifugal stability	Stable	Stable	Stable	Stable	Layered

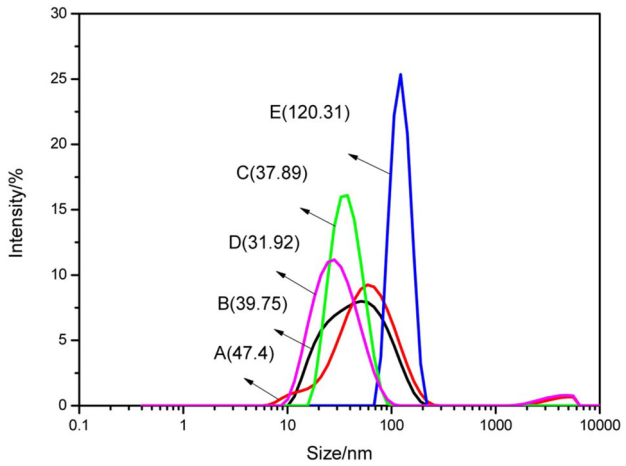

Figure 4 Average particle sizes of PUDs without GAA.

Japan). Antibacterial efficiency of the coatings was calculated by the formula:

$$\text{Antibacterial efficiency}(\%) = \left(\text{OD}^0_{600} - \text{OD}^X_{600}\right)/\text{OD}^0_{600} \times 100\%$$

where OD^0_{600} is the values of the initial ultraviolet peak at 600 nm for blank control bacterial sample and OD^X_{600} is the values for different samples.

Characterization of the coatings

Pencil hardness of coatings was tested by GB/T6739-1996. Adhesion test and the impact resistance were performed according to GB/T9286-1998 and GB/T 1732-1993, separately.

Chemical resistance tests were carried out at room temperature and referred the method of Chaudhari [26].

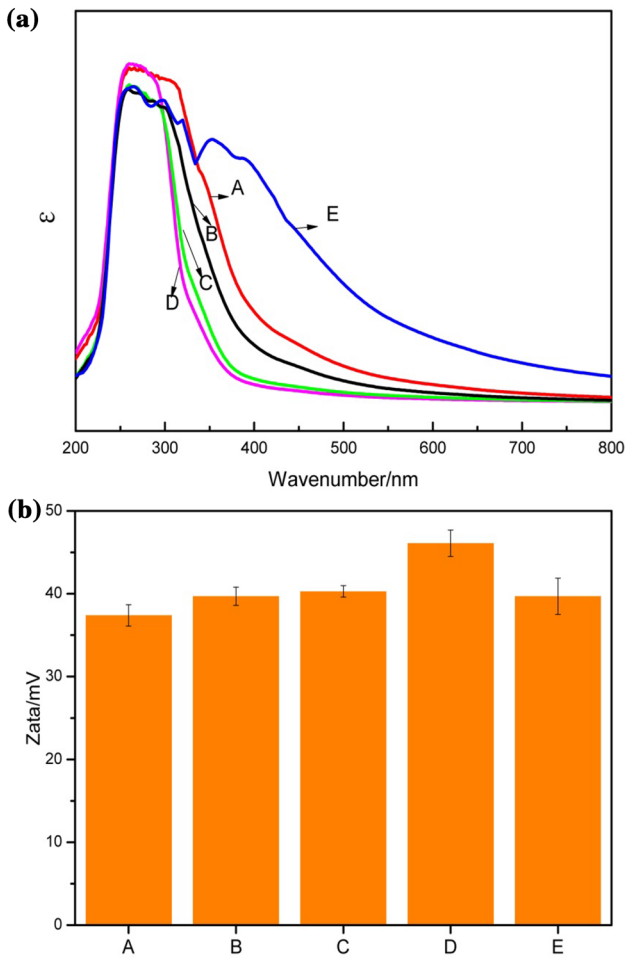

Figure 5 **a** UV–Vis spectrum and **b** zeta potentials of PUDs without GAA.

The contact angle of water on the coatings surface was measured by using CAM (GT-CAMB3, Gentian, China).

The micro-topography of the coatings on the silicon wafer was observed by AFM (MM8, Brucker, USA); the scanning size of the probe is 10 × 10 μm.

The thermal stability of different coatings was studied by the TG-DSC (STA449C, Netzsch, Germany). Samples of 15–20 mg were heated from 25 to 600 °C at a heating rate of 10 °C min^{-1} under argon atmosphere.

The reduced rate of colonies for different coatings was calculated through the equation:

$$\text{Reduced rate of colonies}(\%) = (N_0 - N_X)/N_0 \times 100\%$$

where N_0 is the colonies numbers of the blank control and N_X is the colonies numbers of different coating samples.

Results and discussion

FTIR spectra analysis

The FTIR (FTIR-800S, Shimadzu, Japan) spectra are utilized to determine the material structure and the degree of the reaction. As shown in Fig. 3a, there is no obvious O–H stretching vibration at 3500 cm^{-1}, indicating that –OH of PCL3050 has almost completely reacted. The stretching vibration absorption peak at 3385 cm^{-1} is assigned to –NH–, and the peak at 1722 cm^{-1} belongs to C–O–C (ester bond), which reflecting the formation of urethane groups (–NHCOO–). Meanwhile, the peak at 2270 cm^{-1} ascribed to the characteristic absorption of –NCO is observed [27, 28]. In Fig. 3b, the peak at 2270 cm^{-1} is disappeared, which illustrates that the –NCO has reacted with the –OH completely. The peaks at 1640 and 814 cm^{-1} show the HEMA grafts smoothly, and the peaks of 1090 (C–O–C, ether bond) and 1470 cm^{-1} ($–OCH_3$) are provided by the MPEG, and the peak at 1169 cm^{-1} is classified to the C–N of DMEA. All above results clearly demonstrate the successful synthesis of PWPU. The most obvious changes after curing are displayed in Fig. 3c, where the absorption peaks area decreases drastically at 1640 and 814 cm^{-1}. These changes resulted from the C=C have transformed into the free radicals under the ultraviolet light.

Stability analysis of PUDs

The appearance, storage and centrifugal stability of PUDs with different molar ratios of end-capped agents are shown in Table 2. Previous studies have mentioned that the main factors affecting dispersion stability include the concentration, numbers and location of hydrophilic groups, degree of neutralization and strength of hydrophobic segments [24, 29]. Due to the other factors, we mainly discuss the amine position and strength of hydrophobic segments on dispersion stability.

On the one hand, Table 2 and Fig. 4 display that the PUD-E has the worst stability and the largest particles size (120.31 nm), while the dispersions of PUD-A, B, C and D are more stable and smaller in size (about 40 nm), separately. Since the amine groups located in pendant position of PWPU molecular that brings about the hydrophilic groups exposing adequately so that the entanglement and encapsulation of amine groups in linear chain are prevented. On the other hand, the particle size of PWPU dispersions (PUD-A, B, C, D) reduces as the

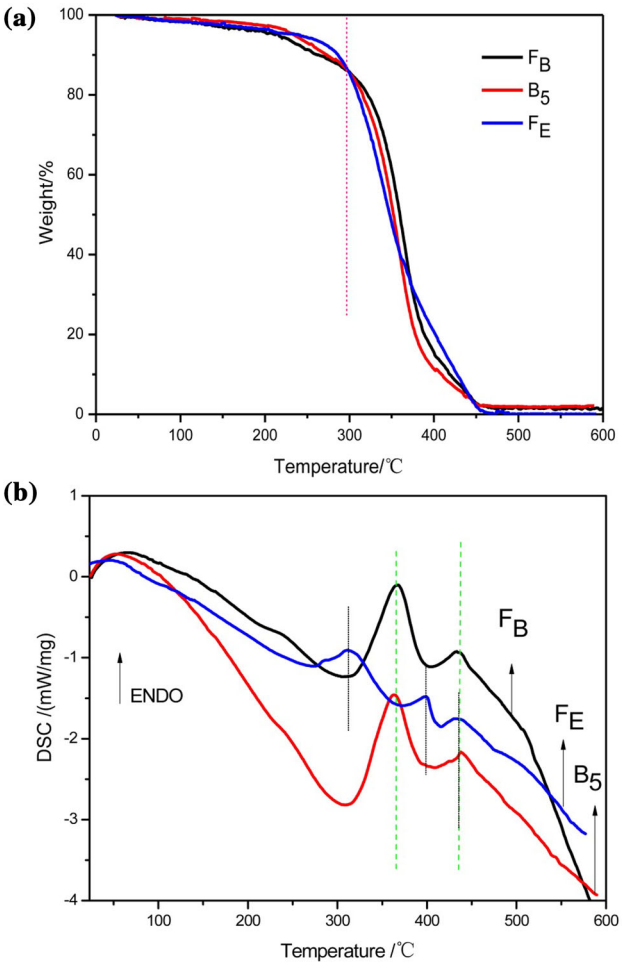

Figure 6 **a** TGA and **b** DSC analyses of F_B, F_E, and B_5.

decrease in the hydrophobic C=C content. When other factors are identical, particle size depends on the strength of hydrophobic segments, because the molecular chains are more easily to entangle and fold for constituting larger particles due to the presence of hydrophobic segments.

UV–Vis spectrum experiments can explain the number of hydrogen bonds [30]. As shown in Fig. 5a, polyurethane acrylate molecule has an absorption peak at around 280 nm, and the half width of PWPU dispersion s is narrower, which demonstrates the particle size of PWPU dispersions is smaller. Consequently, there is less micelles and more opportunities to form hydrogen bonds due to intermolecular collision in the PUD-A, B, C and D. However, when the particle size is too large (PUD-E), there will be more micelles and becoming harder to approach each other due to the electrostatic repulsion. As a result, the hydrogen bonds are reduced, and the stability is deteriorated.

The zeta potentials of all dispersions are above +35 mV in Fig. 5, and the zeta potentials of PWPU dispersions are increased with the promotion of MPEG contents. According to the Stern double-layer model, ions of the Stern layer are in equilibrium with the diffusion layer [31]. When the molecular weight increases with the addition of MPEG, the electrolyte in the dispersion will be reduced that contributes to increasing the thickness of diffusion layer. Afterward, the counterions entered Stern layer will be decreased, resulting in a growth in zeta potential. The difference of the two dispersions in stability further confirms that the amine is successfully grafted to the pendant position of polyurethane chain.

The PUDs accelerated storage experiments at different temperatures were also carried out. The results of Table S1 in electronic supplementary material show the PWPU dispersions still have good stability even at harsh temperatures (0 and 65 °C). A high C=C content sample is more prone to instability at 65 °C, which may be due to the occurrence of free radical polymerization of C=C bonds.

Thermal resistance analysis of coatings

Thermal resistance analysis shows the thermal decomposition of different types and the effects of GAA on coating thermal stability. In Fig. 6a, weight loss of all coatings before 200 °C is resulted from the evaporation of residual water and solvents. The thermal loss of coatings decreases slowly between the 200 and 300 °C, but the declining amplitude of curves greatly increases after 300 °C. Compared with F_B (no GAA), it is found that the weight loss velocity of B_5 increases slightly due to the decomposition of GAA. The upward direction is the endothermic direction, and there exist two major endothermic peaks of PWPU coatings (F_B and B_5) in Fig. 6b. The thermal decomposition of PWPU coatings is divided into two degradation stages, and the inflection point temperatures corresponding to the maximum decomposition rates are about 365 and 440 °C. The thermal degradation stability of the hard segment is lower than that of the soft segment [32]. Thus, the first stage

Table 3 Coating properties tests for polyurethane coatings

Coatings	Appearance	Pencil hardness	Adhesion	Impact resistance	Chemical resistance			
					Water, 168 h	Salt (5% NaCl), 168 h	Acid (5% HCl),120 h	Alkali (5% NaOH), 48 h
F_A	Smooth	2H	0	50 cm	Pass	Pass	Pass	Swells
F_B ($B1$)	Smooth	2H	1	50 cm	Pass	Pass	Pass	Swells
F_C	Smooth, slightly sticky	H	2	50 cm	Pass	Swells	Slightly cracks	Removed
F_D	Rough, sticky	HB	2	50 cm	Swells	Partially removed	Removed	Removed
F_E	Smooth, yellow	3H	0	50 cm	Pass	Pass	Pass	Swells
B_2	Smooth	2H	1	50 cm	Pass	Pass	Pass	Swells
B_3	Smooth	2H	1	50 cm	Pass	Pass	Pass	Swells
B_4	Smooth	2H	1	50 cm	Pass	Pass	Pass	Swells
B_5	Smooth	2H	1	50 cm	Pass	Pass	Swells	Swells

is mainly due to the breakage of relatively weak urethane bonds (–NHCOO–) in the hard segment. The second degradation stage is related to the decomposition of the soft segments that include PCL, MPEG. As the LWPU coatings (F_E), three endothermic peaks are observed at 313, 401 and 440 °C. The endothermic peak noted at 401 °C is probably attributed to the chain extender regent (MDEA) that acts as one part of the hard segment that causes the degradation temperature of the soft segment (PCL) to shift backward. In general, the endothermic and exothermic peaks of PWPU coatings are significantly shifted backward, and the decomposition stage is reduced from 3 to 2. These figures show that the thermal resistance of PWPU coatings is superior to LWPU coatings.

The glass transition temperature (T_g) is also illustrated in Fig S1, whether with or without GAA, the T_g of PWPU coating is higher than that of LWPU. This may be because the whole PWPU molecular chain is more rigid due to its branch structure tending to produce chemical cross-linking and the pendant polar groups of PWPU. However, the LWPU molecular chain has good flexibility and low Tg due to its linear structure. When GAA is introduced at the side of the PWPU molecule, the stiffness of the molecular chain is stronger, resulting in an increase in T_g.

Coating and mechanical properties of the polyurethane coatings

Table 1 shows that the experimental value of Mn is larger than the theoretical value, while the experimental C=C contents and amine values are lower than the theoretical value. This may be due to the fact that some double bonds are polymerized in the synthesis, making Mn larger. The molecular chains are folded or entangled so that some amine groups are buried, which results in lower experimental amine values.

The results of Tables 1 and 3 illustrate that the appearance and most properties of the coatings are

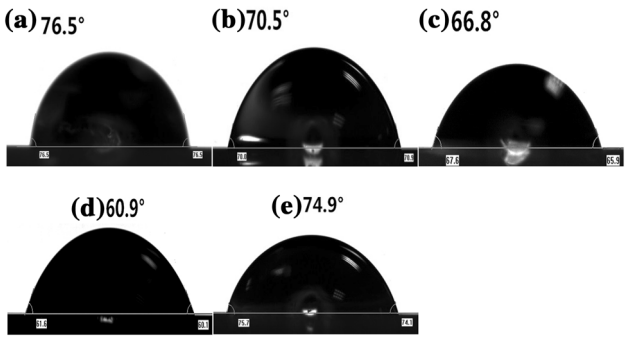

Figure 7 Contact angles of coatings: **a** F_A, **b** F_B, **c** F_C, **d** F_D and **e** F_E.

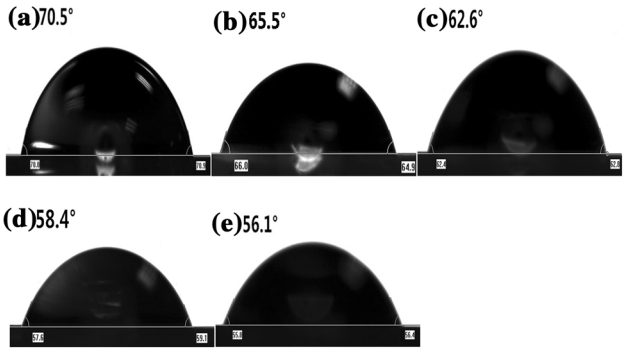

Figure 8 Contact angles of antibacterial coatings with 0, 0.25, 0.5, 0.75 and 1% of GAA: **a** B_1, **b** B_2, **c** B_3, **d** B_4 and **e** B_5.

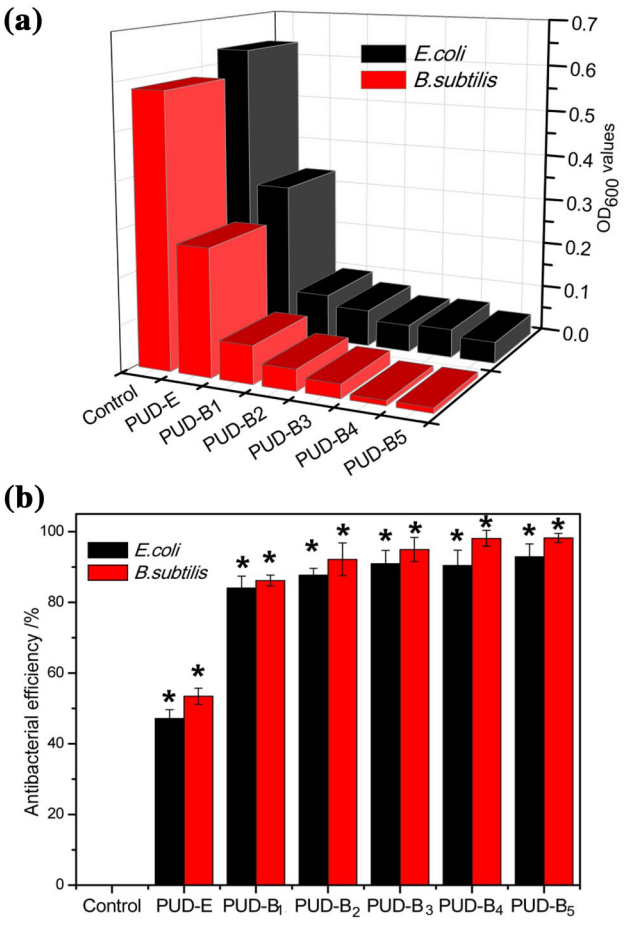

Figure 9 **a** Average OD_{600} values and **b** antibacterial efficiency of the different PUDs. *P represents the statistical significance (P value), *$P < 0.05$.

closely related to the C=C contents [33]. UV curing is a free radical reaction; insufficient C=C will lead the curing reaction to be incomplete. Thus, coatings of F_C and F_D are sticky and rough, in which C=C contents are only 3.645 and 1.781%, respectively. From F_A to F_D, the pencil hardness and degree of adhesion declined 2 levels accompanied by the reduction in C=C contents. In Fig S2, the stress–strain curves are also measured to study the mechanical properties of coatings, and the tensile strength and Young's modulus are summarized in Table S2. With the reduction in C=C contents, the mechanical properties of the coating decreased sharply. Due to the different molecular structure, the coating stress–strain curves of the LWPU and PWPU are completely different, and the LWPU-E with liner molecular has a longer elongation, while the PWPU-A has a stronger tensile strength.

Higher C=C contents play a positive role in the appearance, properties and even chemical resistance of coatings. Different coatings exhibit apparently dissimilar effects on the films when, respectively, immersed in water, salt, acid and alkali for a given time period, whereas in the case of F_C and F_D, coatings partially or totally removed from the substrate are found in liquid. Good chemical resistance of coatings is discovered when the C=C contents are above 5.676%. The sufficient C=C contents lead to a stronger cross-linking network, which causes the shielding for chemicals more powerful. Additionally, the results of impact resistance show that all coatings possess excellent flexibility, and whole tests display that appropriate doses of GAA have little effect on coating properties.

When other factors are same, the coatings of PWPU have dissimilar color with the LWPU. We consider that the PWPU is terminated directly by alcohol amine and this approach supply more effective amine, which can prepare dispersions by using much less amine and acid, thereby preventing the coatings turning yellow due to the abuse of amine.

Hydrophilic research of coatings

Hydrophilic property is critical to biocompatibility of material because the hydrophobic surfaces may cause undesirable biological reactions such as "rejection." The measured hydrophilic results of coatings are presented in Fig. 7, and the contact angle of all coatings to water is less than 90° which demonstrates that the coatings have a hydrophilic surface. Along with the increase in MPEG, the contact angle of the PWPU coatings ($F_{A,\ B,\ C\ \text{and}\ D}$) gradually decreased from 76.5° to 60.9° and a more hydrophilic coating was obtained. If the amine contents and the molecular weight of PWPU-B and LWPU are identical, the

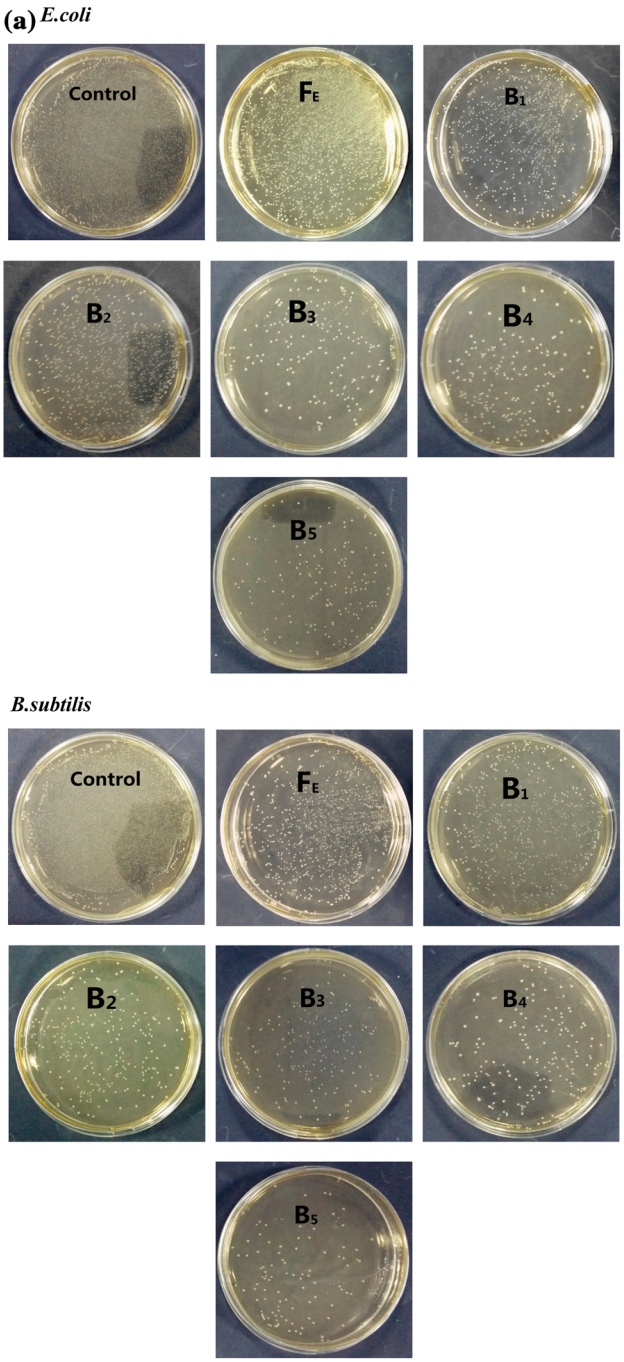

Figure 10 **a** Bacterial colonies photograph of the *E. coli* and *B. subtilis* suspension after incubation with different coatings for 24 h, **b** reduced rates of the *E. coli* and *B. subtilis* colonies for different coatings.

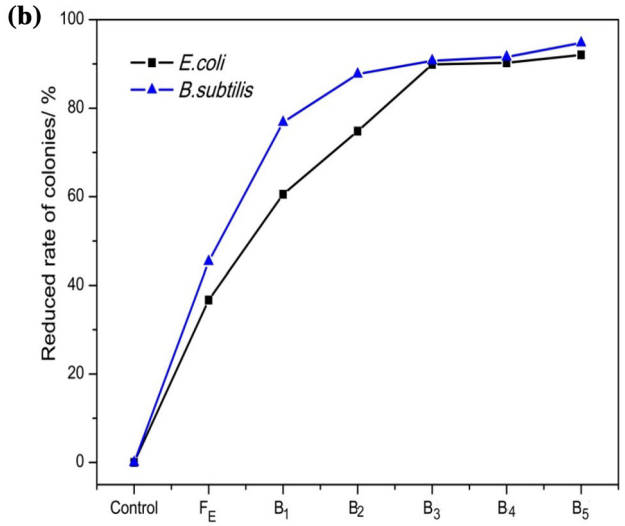

Figure 10 continued.

F_B and F_E should have an equal amount of amine groups in the same region. However, the F_B has a smaller contact angle, manifesting that the hydrophilic groups are more exposed to surface due to the pendant position.

The contact angle of antibacterial coatings with GAA is also measured in Fig. 8. Accompanied by the addition of GAA, the contact angle is declined and the surface becomes more hydrophilic. Adding the GAA is equivalent to enhancing the degree of neutralization, which produces a positive reinforcement in the coating hydrophilicity. These data reflect that the PWPU has biocompatibility and may be applied for the surface in contact with the human body.

Antibacterial properties of PUDs and coatings

Dispersions have unique application in medical, textile and other aspects so that the study of its antibacterial properties is necessary. The results of PUDs are expressed in Fig. 9. On the one hand, the antibacterial efficiency in the *E. coli* tests of PUD-E, PUD-B_1, PUD-B_2, PUD-B_3, PUD-B_4 and PUD-B_5 is 47.16, 84.07, 87.10, 90.93, 90.45 and 92.90%, respectively. On the other hand, there is a similar result in the *B. subtilis* tests, that is, 53.44, 86.16, 92.18, 94.93, 98.10 and 98.20%, separately. The detailed *P values are listed in Table S4 and Table S5, indicating that the data have obviously statistical significance.

The PWPU dispersions have outstanding antibacterial performance against *E. coli* and *B. subtilis*. Particularly, the average antibacterial efficiency of PWPU dispersions (PUD-B_X) is 34.82% higher than that of LWPU (PUD-E) even in the absence of GAA. In the wake of GAA contents increasing from 0 to 1%, the antibacterial efficiency only improved about 10%. Therefore, the antibacterial efficiency of PUDs is mainly attributed to the location of amine groups. The pendant position of PWPU can expose more tertiary amine to form QAS in dispersions. Additionally, the PWPU dispersions have a higher killing efficiency on *B. subtilis*, and it is resulted from the distinction in biofilms of gram-negative and gram-positive bacteria [8].

The bacterial colonies photographs of different coatings are posted in Fig. 10a. The number of *E. coli* colonies is found to be 31.45 CFU cm^{-2} in blank control, LWPU coating (F_E) is 19.91 CFU cm^{-2}, while colonies of PWPU coatings (B_1, B_2, B_3, B_4 and B_5) are 12.41, 7.93, 3.18, 3.07 and 2.50 CFU cm^{-2}. Furthermore, the colonies of *B. subtilis* are 29.44, 16.09, 6.83, 3.62, 2.74, 2.48 and 1.54 CFU cm^{-2}, respectively. Figure 10b shows that the tendency of colonies reduction in coatings is broadly consistent with PUDs, but slightly different. GAA enhances the average antibacterial efficiencies of dispersions and coatings by 10.43 and 24.73%, respectively.

Entire neutralized cationic polyurethane is regarded as a macromolecular QAS, and it can be able to diffuse into every corner of the liquid, so that the character in the dispersion of GAA is not particularly pronounced. However, GAA acts a more significant role on coating surface. Since a portion of QAS is buried after the coating cured, and when GAA is attached to the polyurethane molecule, there will be a QAS with guanidine, and more antibacterial groups are exposed to the coating surface. The fact is confirmed by the images of AFM in Fig. 11; all coating surfaces have several nanometers of undulations, in which the dimmed recesses should be polyester or other hydrophobic segments, and the bright protrusions are hydrophilic segments such as QAS, MPEG. From the morphological results, the amount of protruding parts of B_5 is the most, followed by B_1, and F_E at least. It is noted that the hydrophilic groups of PWPU coatings are more intensive than that of LWPU, and coatings become more hydrophilic after adding the GAA, which is in agreement with the CAM outcomes of Fig. 8. More critically, GAA changes the micro-appearance and increases the number of arrow-shaped portions forasmuch dense

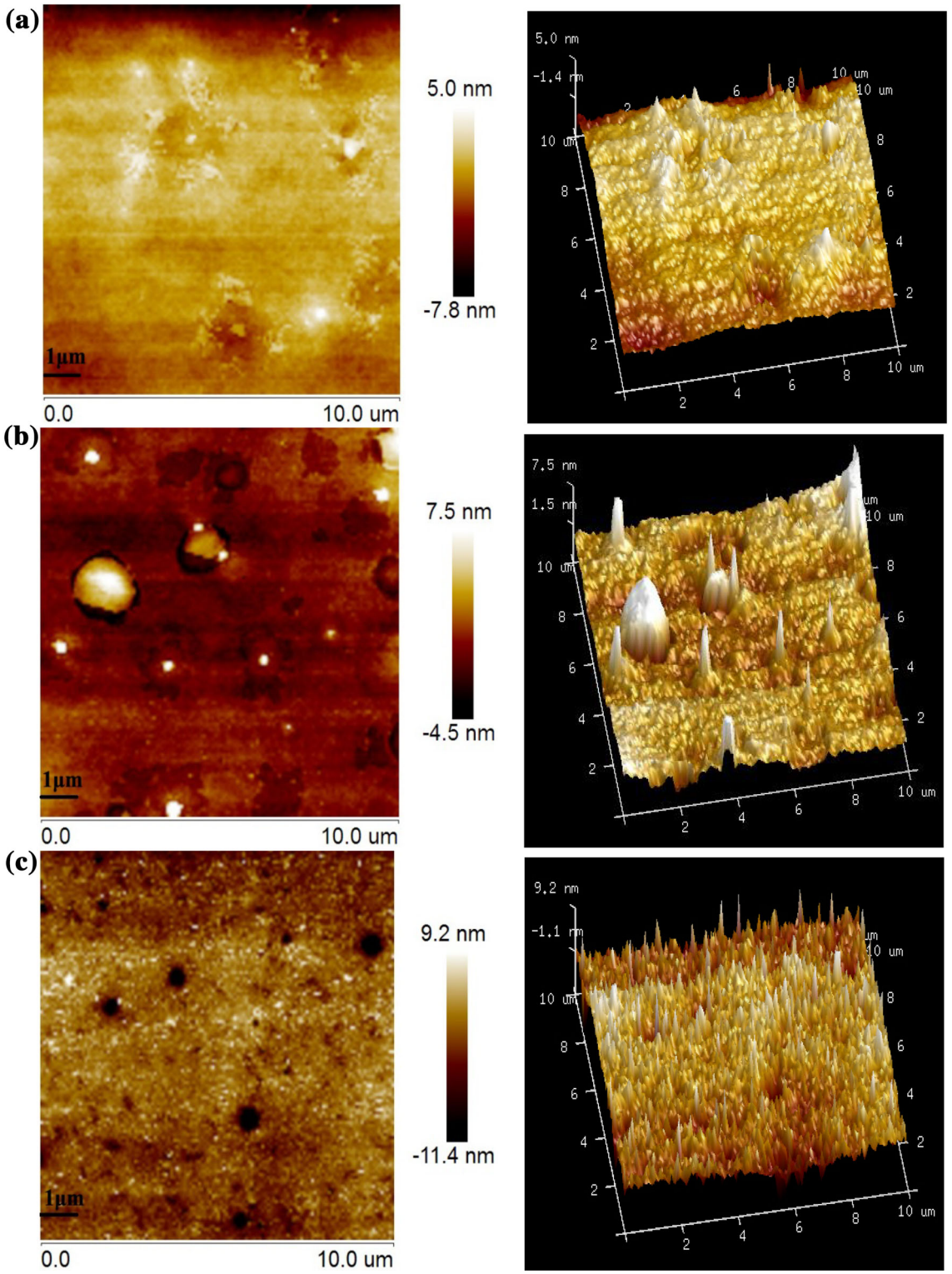

Figure 11 AFM images of coatings for **a** F_E, **b** B_1 and **c** B_5.

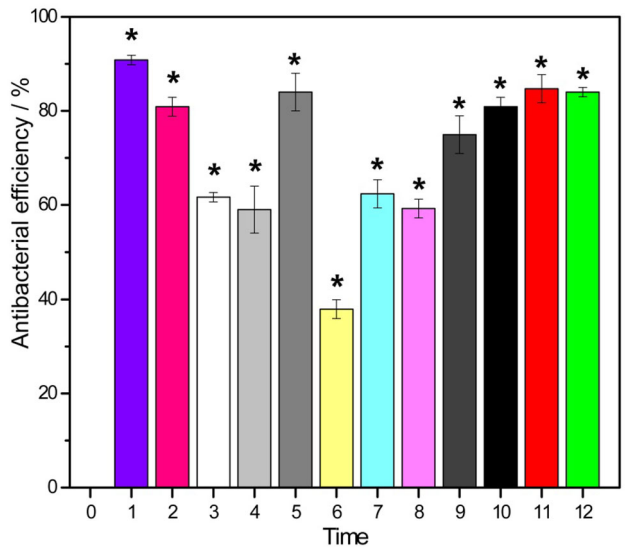

Figure 12 Outcomes of repeat antibacterial challenge tests for *B. subtilis* on B_5 coating. $^*P < 0.05$.

and sharp arrows are more possibly to pierce the cell biofilm when bacteria contact the surface.

The repeat antibacterial challenge tests

Figure 12 shows the outcomes of repeat antibacterial challenge tests of B_5 coating which is washed with running water every 4 h, and the antibacterial efficiency of coating has a tortuous change after washing. At the first time, the antibacterial parts kill most (94.77%) of the bacteria on coating surface. The antibacterial efficiency declines after cleaning, but a peak of antibacterial efficiency appears again at the fifth time. We speculate that the contact between the bactericidal groups and new bacteria is hindered by the dead bacteria absorbed on coating surface. The antibacterial efficiency quickly recovers after the sixth time as the prolonging of flushing times and reaches a steady level in the last two tests. The optical microscope photograph of *B. subtilis* washed with water after each repeat antibacterial test is shown in Fig S3. This trend reflects that the dead bacterium adsorbed on coating surface has been removed by repeated washing, and the reduction in final antibacterial efficiency is due to the emergence of partial GAA dissolution after repeat laundering. Fortunately, the antibacterial efficiency can remain at 87.94% after 12 times washing. It demonstrates that the major antibacterial compositions of polyurethane coatings are not attenuated greatly as the increase in the application times.

The antibacterial principle of coatings

The PWPU is a bactericidal polymer according to the classification of Siedenbiedel, and the function is produced by the synergistic effects of its structure [7]. Based on the above results, a possible mechanism schematically is proposed and illustrated in Fig. 13. After forming the coatings, MPEG fragments of

Figure 13 Schematic diagram of antibacterial principle.

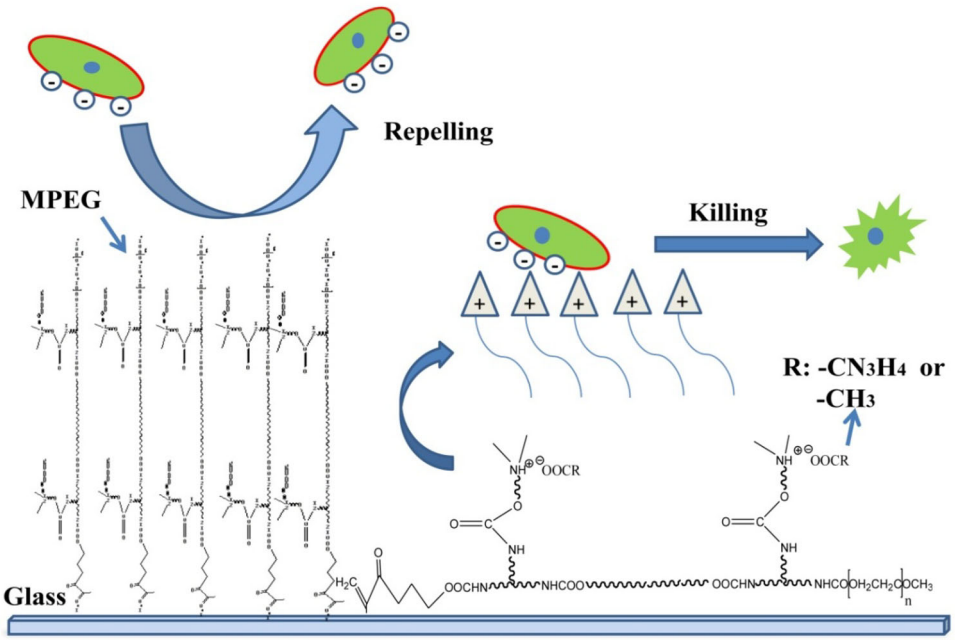

molecular construct a huge network, which generates a great steric hindrance to repel bacteria. Moreover, guanidine and amino groups carry powerful positive charge, and GAA is linked on polyurethane molecules to form a QAS with guanidine, which creates a double reinforced positive charge. Due to the production of double hydrogen bonding between the phospholipid layers and guanidine, the combinations of QAS and bacteria are more firm and the contact chances are greatly enlarged. The arrowhead-like antibacterial parts develop a strong electrostatic interaction to the residual negatively charged bacteria and destroy the cell walls to make the cytoplasm flows out, leading to bacterial death. There is no target–target-specific binding between coatings and bacteria; wherefore, the drug resistance is very diminutive. Meanwhile, the outer layer of mammalian cell is electrically neutral, which causes the PWPU harmless to human [3].

Conclusions

In this work, a simple method of manufacturing PWPU and modifying with GAA to obtain self-antibacterial material was provided. Attributed to the pendant amine, the dispersion is particularly steady and the coating thermal resistance is improved. The coating has superior antibacterial property, which is indicated by a 94.77% killing efficiency even for a 4-h culture due to the benefits of pendant amine and GAA. Furthermore, a more hydrophilic PWPU coating owns more powerful antibacterial performance and the GAA-modified effect of coatings is better than that of dispersions. The antibacterial efficiency reduces only 6.82% after 12 times washing, which reveals the excellent reproducibility of PWPU coatings. Considering all aspects, we recommend the PWPU-B as the best comprehensive schemes for preparing resin and the dosage of GAA should be 1% (wt. of the dispersions). Overall, this research has large potential in antibacterial coating materials.

Acknowledgements

The authors would like to thank the financial support from the Major Science and Technology Projects of Hunan Province, China (2015GK1004). Thanks to Prof. Shengpei Su of Hunan Normal University for his warm help and guidance.

Compliance with ethical standards

Conflict of interest The authors declare that we have no conflict of interest.

Electronic supplementary material: The online version of this article (doi:10.1007/s10853-017-1527-2) contains supplementary material, which is available to authorized users.

References

[1] Fuchs AD, Tiller JC (2006) Contact-active antimicrobial coatings derived from aqueous suspensions. Angew Chem Int Ed 45:6759–6762

[2] Kumar M, Bala R, Gondil VS, Pandey SK, Chhibber S, Jain DVS, Sharma RK, Wangoo N (2017) Combating food pathogens using sodium benzoate functionalized silver nanoparticles: synthesis, characterization and antimicrobial evaluation. J Mater Sci. doi:10.1007/s10853-017-1072-z

[3] Wynne JH, Fulmer PA, McCluskey DM, Mackey NM, Buchanan JP (2011) Synthesis and development of a multifunctional self-decontaminating polyurethane coating. ACS Appl Mater Interfaces 3:2005–2011

[4] Xu X, Zheng AN, Zhou XD, Guan Y, Pan YF, Xiao HN (2015) Antimicrobial polyethylene wax emulsion and its application on active paper-based packaging material. J Appl Polym Sci 132(27). doi:10.1002/app.42214

[5] Huang YH, Chen MHC, Lee BH, Hsieh KH, Tu YK, Lin JJ, Chang CH (2014) Evenly distributed thin-film Ag coating on stainless plate by tricomponent Ag/Silicate/PU with antimicrobial and biocompatible properties. ACS Appl Mater Interfaces 6:20324–20333

[6] Timofeeva L, Kleshcheva N (2011) Antimicrobial polymers: mechanism of action, factors of activity, and applications. Appl Microbiol Biotechnol 89:475–492

[7] Siedenbiedel F, Tiller JC (2012) Antimicrobial polymers in solution and on surfaces: overview and functional principles. Polymers 4:46–71

[8] Liu K, Su ZG, Miao SD, Ma GH, Zhang SP (2016) UV-curable enzymatic antibacterial waterborne polyurethane coating. Biochem Eng J 113:107–113

[9] Kugimoto Y, Wakabayashi A, Dobashi T, Ohnishi O, Doi TK, Kurokawa S (2016) Preparation and characterization of composite coatings containing a quaternary ammonium salt as an anti-static agent. Prog Org Coat 92:80–84

[10] Toker RD, Apohan NK, Kahraman MV (2013) UV-curable nano-silver containing polyurethane based organic–inorganic hybrid coatings. Prog Org Coat 76:1243–1250

[11] Li JH, Hong RY, Li MY, Li HZ, Zheng Y, Ding J (2009) Effects of ZnO nanoparticles on the mechanical and antibacterial properties of polyurethane coatings. Prog Org Coat 64:504–509

[12] Tiller JC, Liao CJ, Lewis K, Klibanov AM (2001) Designing surfaces that kill bacteria on contact. Proc Natl Acad Sci USA 98:5981–5985

[13] Garrison TF, Zhang ZY, Kim HJ, Mitra D, Xia Y, Pfister DP, Brehm-Stecher BF, Larock RC, Kessler MR (2014) Thermomechanical and antibacterial properties of soybean oil-based cationic polyurethane coatings: effects of amine ratio and degree of crosslinking. Macromol Mater Eng 299: 1042–1051

[14] Ho CH, Tobis J, Sprich C, Thomann R, Tiller JC (2004) Nanoseparated polymeric networks with multiple antimicrobial properties. Adv Mater 16:957–961

[15] Liu GF, Wu GM, Jin C, Kong ZW (2015) Preparation and antimicrobial activity of terpene-based polyurethane coatings with carbamate group-containing quaternary ammonium salts. Prog Org Coat 80:150–155

[16] Grapski JA, Cooper SL (2001) Synthesis and characterization of non-leaching biocidal polyurethanes. Biomaterials 22:2239–2246

[17] Wei DF, Ma QX, Guan Y, Hu FZ, Zheng A, Zhang X, Teng Z, Jiang H (2009) Structural characterization and antibacterial activity of oligoguanidine (polyhexamethylene guanidine hydrochloride). Mater Sci Eng C 29:1776–1780

[18] Wender PA, Galliher WC, Goun EA, Jones LR, Pillow TH (2008) The design of guanidinium-rich transporters and their internalization mechanisms. Adv Drug Deliv Rev 60:452–472

[19] Mattheis C, Wang H, Meister C, Agarwal S (2013) Effect of guanidinylation on the properties of poly (2-aminoethylmethacrylate)-based antibacterial materials. Macromol Biosci 13:242–255

[20] Michl TD, Locock KES, Stevens NE, Hayball JD, Vasilev K, Postma A, Qu Y, Traven A, Haeussler M, Meagherb L, Griesserd HJ (2014) RAFT-derived antimicrobial polymethacrylates: elucidating the impact of end-groups on activity and cytotoxicity. Polym Chem 5:5813–5822

[21] Fischer M, Vahdatzadeh M, Konradi RT, Friedrichs J, Maitz MF, Freudenberg U, Werner C (2015) Multilayer hydrogel coatings to combine hemocompatibility and antimicrobial activity. Biomaterials 56:198–205

[22] Qin LL, He Y, Liu BH, Jian Y, Li CG, Nie J (2013) Preparation and properties of polyurethane acrylates modified by saturated alcohols. Prog Org Coat 76:1594–1599

[23] Fang ZH, Duan HY, Zhang ZH, Wang J, Li DQ, Huang YX, Shang JJ, Liu ZY (2011) Novel heat-resistance UV curable waterborne polyurethane coatings modified by Melamine. Appl Surf Sci 257:4765–4768

[24] Pan XJ, Sun DC (2015) Novel cationic UV-curable cathodic electrophoretic coatings with pendant amine salt. J Chem Ind Eng 66:4696–4702

[25] Dilger RN, Angeloni KB, Payne RL, Lemme A, Parsons CM (2013) Dietary guanidino acetic acid is an efficacious replacement for arginine for young chicks. Poult Sci 12:171–177

[26] Chaudhari AB, Tatiya PD, Hedaoo RK, Kulkarni RD, Gite VV (2013) Polyurethane prepared from neem oil polyesteramides for self-healing anticorrosive coatings. Ind Eng Chem Res 52:10189–10197

[27] Llorente O, Fernández-Berridi MJ, González A, Irusta L (2016) Study of the crosslinking process of waterborne UV curable polyurethane acrylates. Prog Org Coat 99:437–442

[28] Xu JC, Rong XS, Chi TY, Wang M, Wang YY, Yang DY, Qiu FX (2013) Preparation, characterization of UV-curable waterborne polyurethane acrylate and the application in metal iron surface protection. J Appl Polym Sci 130: 3142–3152

[29] Madbouly SA, Otaigbe JU, Nanda AK, Wicks DA (2005) Rheological behavior of aqueous polyurethane dispersions: effects of solid content, degree of neutralization, chain extension, and temperature. Macromolecules 38:4014–4023

[30] Lu ZQ, Zhu YY, Lin JB, Jiang XK, Li ZT (2010) Hydrogen bonded foldamer-bridged biscoumarins: a UV-Vis absorption and fluorescent study of the solvent effect. Chin Sci Bull 55:2870–2878

[31] López-García JJ, Grosse C, Horno J (2009) On the use of the Stern-layer and the charged-layer formalisms for the interpretation of dielectric and electrokinetic properties of colloidal suspensions. J Colloid Interface Sci 329:384–389

[32] Liu K, Miao SD, Su ZG, Sun LJ, Ma GH, Zhang SP (2016) Castor oil-based waterborne polyurethanes with tunable properties and excellent biocompatibility. Eur J Lipid Sci Technol 118:1512–1520

[33] Zhang T, Wu WJ, Wang XJ, Mu YP (2010) Effect of average functionality on properties of UV-curable waterborne polyurethane-acrylate. Prog Org Coat 68:201–207